Broadband omnidirectional antireflection coatings optimized by genetic algorithm

David J. Poxson,[1] Martin F. Schubert,[2] Frank W. Mont,[2] E. F. Schubert,[1,2] and Jong Kyu Kim[2,*]

[1]*Department of Physics, Applied Physics, and Astronomy, Future Chips Constellation, Rensselaer Polytechnic Institute, Troy, New York 12180, USA*

[2]*Department of Electrical, Computer, and Systems Engineering, Future Chips Constellation, Rensselaer Polytechnic Institute, Troy, New York 12180, USA*

**Corresponding author: Kimj4@rpi.edu*

Received December 11, 2008; revised January 14, 2009; accepted January 26, 2009; posted February 3, 2009 (Doc. ID 105212); published March 5, 2009

An optimized graded-refractive-index (GRIN) antireflection (AR) coating with broadband and omnidirectional characteristics—as desired for solar cell applications—designed by a genetic algorithm is presented. The optimized three-layer GRIN AR coating consists of a dense TiO_2 and two nanoporous SiO_2 layers fabricated using oblique-angle deposition. The normal incidence reflectance of the three-layer GRIN AR coating averaged between 400 and 700 nm is 3.9%, which is 37% lower than that of a conventional single-layer Si_3N_4 coating. Furthermore, measured reflection over the 410–740 nm range and wide incident angles 40°–80° is reduced by 73% in comparison with the single-layer Si_3N_4 coating, clearly showing enhanced omnidirectionality and broadband characteristics of the optimized three-layer GRIN AR coating.

OCIS codes: 310.1210, 310.4165, 220.4241.

Antireflection (AR) coatings are used extensively in a wide variety of optical systems to reduce unwanted reflections. AR coatings for solar cells are particularly important, because reducing reflection at the surface of solar cells directly increases efficiency and, hence, helps solve today's energy crisis. Conventional AR coatings for solar cells consist of single-layer quarter-wave transparent films that provide excellent AR characteristics at the designed wavelength and normal incidence. However, performance of such quarter-wave coatings falls off when deviating from normal incidence or the designed wavelength. Because sunlight is inherently broadband and its angle of incidence changes throughout the day, broadband and omnidirectional AR characteristics are highly desirable for solar cell devices.

The concept of graded-refractive-index (GRIN) AR coatings with broadband and omnidirectional characteristics was conceived over a century ago [1]. Several continuous design methodologies and implementation by using nanoporous materials have been published on high-performance broadband GRIN AR coatings [2–5]. Recently, a step-graded GRIN AR coating that virtually eliminates Fresnel reflections, enabled by a new class of optical thin film materials with a refractive index as low as 1.05, has been demonstrated [6]. Subsequent implementations have used step-graded quintic or Gaussian profile AR coatings for use with light-emitting diodes [7] and solar cell applications [8]. However, limitations exist in achieving optimum AR characteristics from quintic and Gaussian profiles. (i) Such profiles are fixed designs, where there is no room for considering important parameters, such as refractive-index dispersion of coating and substrate materials, spectral distribution of incident light, and responsivity of devices, etc. for application-specific optimization. (ii) These profiles require high-refractive-index (high-n) transparent materials—which often do not exist—to grade the refractive index continuously from a high-n substrate, such as silicon, to a low-n ambient medium. If this condition is not met, AR performance is significantly reduced. (iii) In practice, implementing such continuous GRIN profiles is problematic. The quintic and Gaussian profiles may be approximated by dividing the continuous profiles into multiple discrete layers; this, however, does not give the optimum performance. Recently, a computational genetic algorithm method was demonstrated to design optimized GRIN profiles for AR coatings [9] enjoying key advantages over quintic and Gaussian profiles. Unlike the quintic and Gaussian profiles, the genetic algorithm is an optimization design method with which any figure of merit can be taken into consideration. Using the concepts borrowed from biology, namely, selection, mutation, and combination, optimized AR films can be designed. Furthermore, the genetic algorithm method is a practical and application-specific optimization method because factors, such as material availability, angles of incidence, device responsivity curves, and relative weighting of the solar spectrum, can be considered to achieve an optimum performance in a specific condition.

A GRIN AR coating on a silicon substrate is designed using the iterative genetic algorithm computational method [9]. In the implementation of the genetic algorithm, a large population of AR structures is randomly generated. Each structure is tested for "fitness" based on a figure of merit. A small percentage of the worst performing structures is discarded, to be replaced by crossover and mutation of a randomly selected pair of the remaining fit structures. The genetic algorithm process is an iterative method that is repeated until good convergence on an optimized structure, in terms of thickness and refractive index of each layer, is achieved. The figure of merit for these calculations was chosen to be average reflectance, R_{ave},

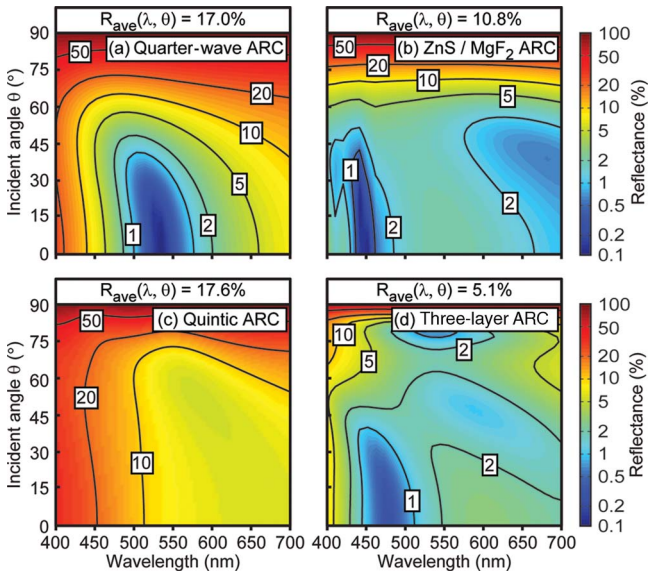

Fig. 1. (Color online) Simulated reflection characteristics of AR coatings. (a) Traditional single-layer quarter-wave AR coating, (b) ZnS/MgF_2 bilayer AR coating, (c) continuous quintic AR coating, and (d) three-layer GRIN AR coating as a function of wavelength and incident angle.

$$R_{\text{ave}} = \frac{1}{\lambda_2 - \lambda_1}\frac{2}{\pi}\int_{\lambda_1}^{\lambda_2}\int_{0}^{\pi/2}\frac{R_{\text{TE}}(\lambda,\theta) + R_{\text{TM}}(\lambda,\theta)}{2}\mathrm{d}\theta\mathrm{d}\lambda, \tag{1}$$

with equal weighting for the wavelength range of 400–700 nm and angles 0°–90°, where R_{TE} and R_{TM} are the angle and the wavelength-dependent reflection coefficients for TE- and TM-polarized light modes. Dense TiO_2 is chosen as the first layer on the Si substrate owing to its high-n and transparency. Since the use of a final layer with a refractive index close to that of air can greatly reduce reflection, porous SiO_2 with a refractive index of 1.05 is chosen as the last layer. Refractive index dispersion curves measured by ellipsometry for TiO_2 and low-n SiO_2 materials are used in these optimization calculations. The resulting optimized design is summarized in Table 1. The optimized GRIN AR coating structure consists of three layers with a 105-nm-thick porous SiO_2 layer, with a refractive index of 1.35 as the second layer. Further calculations of structures with four or more layers result in negligible performance enhancements.

Figures 1(a)–1(d) show a calculated reflectance of an optimized single-layer quarter-wave, bilayer continuous quintic, and the genetic algorithm optimized three-layer GRIN AR coatings, respectively, as a function of wavelength and incident angle. Quintic profile calculations use the same total thickness, 497 nm, and the same upper and lower boundaries for refractive index as the three-layer GRIN AR coating. The quarter-wave coating is calculated with a thickness of 68.4 nm and a refractive index of 1.95. An optimized bilayer ZnS/MgF_2 AR coating [10] is calculated with layer thicknesses of 52.0 and 107.8 nm, respectively. The three-layer GRIN AR coating shows a significant reduction in reflectance over a wide range of incident angles and wavelengths in comparison with traditional quarter-wave, bilayer AR, and continuous quintic AR coatings. The calculated average reflectance R_{ave}, over the wavelength range of 400–700 nm and incident angles from 0° to 90°, is summarized in Fig. 1. We note that the performance of this quintic AR coating is limited by the lack of available transparent high-n materials close to that of a silicon substrate, the nonoptimized choice in coating thickness, and the chosen wavelength range.

To experimentally demonstrate the viability of such a design, the three-layer GRIN AR coating in Table 1 was fabricated. The first layer of TiO_2 was deposited with an rf magnetron sputtering source on a silicon substrate. The deposition rate was controlled by the power supplied to the TiO_2 target and the deposition time. The second and the third layers of porous SiO_2 were deposited using oblique-angle electron-beam evaporation. Utilizing a recently identified analytic formula for porosity and growth rate for the oblique-angle evaporation of nanoporous films [11], the deposition angle of each layer was determined for achieving a desired refractive index and thickness. Based on the analytic formula, the second layer of SiO_2 with 24% porosity was deposited at a 55° deposition angle, followed by the deposition of a low-n SiO_2 layer with 90% porosity at an 85° deposition angle. The thickness and the refractive index of each layer were measured using ellipsometry.

A scanning electron micrograph (SEM) of the three-layer GRIN AR coating is shown in Fig. 2. The first layer is a 49-nm-thick bulk TiO_2. The second layer consists of 99 nm of SiO_2 with a porosity of 24% and has an appearance similar to that of bulk films. The third layer consists of 360 nm of SiO_2 with a porosity of 90%. As shown in Table 1, excellent agreement between optimized design values and experimentally acquired ones, both in terms of thickness and refractive index, is realized. For comparison purposes, a conventional single-layer Si_3N_4 AR coating

Table 1. Thickness and Refractive Index of Each Layer in the Optimized Three-Layer GRIN AR Coating, Designed by Genetic Algorithm, and Measured by Ellipsometry After Fabrication

		Thickness (nm)		Refractive Index (n)	
Layer	Material	Designed	Measured	Designed	Measured
1	TiO_2	49.3	48.8	2.37	2.37
2	SiO_2 24% Porosity	105.1	98.6	1.35	1.40
3	SiO_2 90% Porosity	343.2	360.0	1.05	1.05

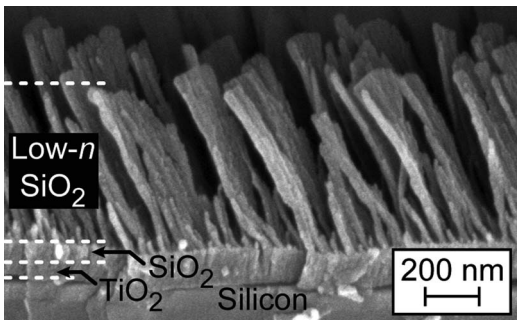

Fig. 2. SEM with a tilt angle of 44° of three-layer GRIN AR coating.

was also fabricated. For this quarter-wave coating, the measured refractive index and thickness is 1.93 and 74 nm, respectively.

Next, we compare both calculated and measured average reflectance for the three-layer GRIN AR coating against a conventional single-layer Si_3N_4 quarter-wave coating. At first, let us consider normal incidence reflectance over the 400–700 nm wavelength range. The reflectance of the single-layer Si_3N_4 AR coating is measured to be near 0 at the designed wavelength, 550 nm, which shows that the quarter-wave AR coating works well as designed. However, measurements confirm that reflectance increases significantly when deviating from 550 nm. The reflectance of the three-layer GRIN AR coating maintains low reflectance, less than 5%, over the entire 400–700 nm wavelength range, demonstrating strong broadband characteristics. The averaged normal incidence reflectance of the three-layer GRIN AR coating is 3.9%, corresponding to a 37% reduction over that of the single-layer Si_3N_4 AR coating. Second, let us consider omnidirectional characteristics of the AR coatings measured over the incident angle range of 40°–80°. Figure 3 shows both measured and calculated angular reflectance of the single-layer Si_3N_4 AR coating and the three-layer GRIN AR coating averaged over the incident angle range of 40°–80° as a function of wavelength. Calculated and measured curves are in good agreement. These measurements correspond to a calculated decrease in average reflection from 22.4% for the single-layer AR coating to 6.1% for the three-layer GRIN AR coating. This 73% reduction in average reflectance further highlights the importance of AR coatings with both omnidirectionality and broadband characteristics. Although our reflectance measurements of the three-layer GRIN AR coating showed a birefringence effect, parallel versus perpendicular average angular reflectance measurements resulted in a 0.5% difference, considered negligible given the overall decrease in reflectance.

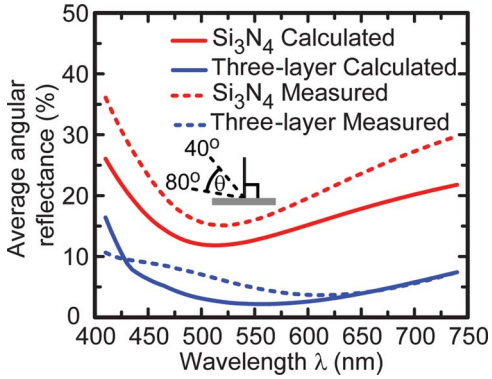

Fig. 3. (Color online) Comparison of the quarter-wave AR coating versus the three-layer GRIN AR coating over angle of incidence 40°–80° and wavelength range 410–740 nm.

In conclusion, we used the computational genetic algorithm method to develop an optimized AR coating with broadband and omnidirectional characteristics. Simulations of the optimized three-layer GRIN AR coating predict significant performance increases when compared to conventional quarter-wave or quintic AR coatings. The three-layer GRIN AR design has been fabricated, and reflectance measurements have shown excellent agreement between simulation and experiment. These reflectance measurements have shown a remarkable reduction in reflectance over the optimized wavelength range of 400–700 nm. Furthermore, measurements for angular reflectance of incident light from 40° to 80° indicate the three-layer GRIN AR coating's strong omnidirectional characteristics.

The authors acknowledge support through the National Science Foundation (NSF) Smart Lighting Engineering Research Center (EEC-0812056) the Nanoscale Science and Engineering Center for Directed Assembly of Nanostructures (DMR-0642573), Sandia National Laboratories, Department of Energy, Crystal IS, Magnolia Optics, Samsung Electro-Mechanics Company, Troy Research Corporation, and New York State.

References

1. S. J. Rayleigh, Proc. London Math. Soc. **11**, 51 (1880).
2. W. H. Southwell, Opt. Lett. **8**, 584 (1983).
3. D. Poitras and J. A. Dobrowolski, Appl. Opt. **43**, 1286 (2004).
4. M. Chen, H. Chang, A. S. P. Chang, S.-Y. Lin, J.-Q. Xi, and E. F. Schubert, Appl. Opt. **46**, 6533 (2007).
5. S. R. Kennedy and M. J. Brett, Appl. Opt. **42**, 4573 (2003).
6. J.-Q. Xi, M. F. Schubert, J. K. Kim, E. F. Schubert, M. Chen, S.-Y. Lin, W. Liu, and J. A. Smart, Nat. Photonics **1**, 176 (2007).
7. J. K. Kim, S. Chhajed, M. F. Schubert, E. F. Schubert, A. J. Fischer, M. H. Crawford, J. Cho, H. Kim, and C. Sone, J. Adv. Mater. **20**, 801 (2008).
8. M.-L. Kuo, D. J. Poxson, Y. S. Kim, F. W. Mont, J. K. Kim, E. F. Schubert, and S.-Y. Lin, Opt. Lett. **33**, 2527 (2008).
9. M. F. Schubert, F. W. Mont, S. Chhajed, D. J. Poxson, J. K. Kim, and E. F. Schubert, Opt. Express **16**, 5290 (2008).
10. E. H. Hect, *Optics* (Addison-Wesley, 2002), p. 429.
11. D. J. Poxson, F. W. Mont, M. F. Schubert, J. K. Kim, and E. F. Schubert, Appl. Phys. Lett. **93**, 101914 (2008).